Evaluation of fatigue property of PET tyre cord and rubber by using thermoluminescence

LIANG BAO LIU, MASAO SUMITA, KEIZO MIYASAKA
Department of Textile and Polymeric Materials, Tokyo Institute of Technology, Ookayama, Meguro-ku, Tokyo 152, Japan

The experimental analysis of thermoluminescence (TL) activation energy, E, and frequency factor, S, by changing heating rate was applied to the investigations of fatigue and fatigue resistance performances of poly(ethylene terephthalate) (PET) tyre cords and tyre rubber. The TL frequency factor, S, was found to be very sensitive to the process of the fatigue of the PET cords and rubber sheet. A strong correlation between TL frequency factor and fatigue process was found which is expected to be applied as a new approach to the studies of fatigue in polymers.

1. Introduction

As the use of polymers in engineering applications has risen in the past decades, an increasing amount of attention has been devoted to their performance and behaviour under cyclic loading conditions. Under cyclic loads polymers will fail at stress levels much lower than they can withstand under monotonic static conditions. It is therefore of considerable technological interest to improve the resistance of polymer to fatigue failure. To do this it is first necessary to understand the mechanisms involved in the fatigue failure of polymers in service. Also, knowledge and understanding are needed of the characterization of structural changes in the process of fatigue, and of the suitable fine structure which has the potential for good fatigue resistance performance. Many polymer scientists, therefore, have made efforts in recent years to address the question of what structure is suitable for cyclic loading in practice.

Of all the works concerning the mechanism of fatigue polymers, the hysteresis model originating from the research of Feltner and Morrow [1] for inorganic materials should be mentioned first, in which they postulated an energy criterion for fatigue failure, and assumed microplastic strain hysteresis energy as an index for fatigue damage. On this basis, they developed a relation between stress amplitude and the number of cycles to failure which utilizes only material properties obtained from the static true stress–strain tension test. A few more investigations which essentially followed the same concepts as those mentioned above, but for polymers, can be found in the literature [2, 3].

Another approach, which is rather more popular than any other, is phenomenalistic studies in which the formation of crazes and cracks is considered to be the essential cause of fatigue failure in most polymers [4, 5], but this is effective only in the final stage of the fatigue process of a material and therefore is confined only to such a situation in which the crazes and cracks are so distinct that they can be observed by, for example, the scanning electron microscope. Recently, a quite promising approach which has involved molecular considerations, including that of viscoelastic properties of polymers, has been attempted, the recent progress of which can be found in an excellent review by Kajiyama [6]. These studies showed that the viscoelastic behaviour of polymeric materials under cyclic loads was correlated with the fatigue behaviour. However, further examination into the above studies leads us to conclude that a more microscopic consideration is necessary to understand the fatigue behaviour of polymeric materials under cyclic loads. Unfortunately, few investigations of this kind have been performed so far. This may be due to the fact that the ordinary approaches of polymer research such as wide- and small-angle X-ray diffraction, birefringence, infrared spectroscopy, etc., are difficult for identifying the structural changes of polymers in the process of fatigue.

We try to establish a new way to evaluate the fatigue resistance properties of these polymers, and an approach by means of thermoluminescence (TL) is developed in this study to characterize the performance and behaviour of polymers under fatigue. In our previous papers [7, 8] we reported that the TL method was effective for the characterization of PET fibres and films, and the results indicated the possibility of using the TL method for the evaluation of the fatigue resistance properties of polymers.

2. Experiments and sample preparations
2.1. Samples
Poly(ethylene terephthalate) (PET) tyre cords have an excellent combination of strength, high modulus, fatigue resistance and dimensional stability, so that polyester has assumed a leading position as carcass fabric for passenger tyres. However, great strength losses in service, especially at high temperature, still remains [9]. Many investigations concerning the

TABLE I Materials and treatments

Sample name	Sample no.	Treatment method
PET cord	1	Original cord
	2	Heat set cord*
	3	Dipped cord†
	4	Fatigued dipped cord
Tyre Rubber (NR/SBR)	5	Vulcanized (168°C, 15 min)
	6	Vulcanized (168°C, 60 min)
	7	Vulcanized (168°C, 120 min)
	8	Fatigued rubber for carcass

*Dried at 130°C for 180 sec and set at 240°C for 120 sec.
† Dipped in adhesive liquid after heat set treatment.

fatigue performances of polyester tyre cords revealed that these strength losses generally attributed to a complex result of both mechanical fatigue and chemical degradation. The examination of the investigations of the fatigue of PET cords [10, 11] shows that they are limited to the phenomenalistic levels as before, and thus it is still necessary to elucidate the fatigue process of PET tyre cords.

In this study, PET tyre cords in different states, as well as tyre rubber sheet provided by courtesy of Yokohama Rubber Co., Japan, were used as the samples. The tyre rubber sheet is a blend of NR and SBR with a volume fraction of about 50% for NR and SBR, respectively. The treatment methods and the mechanical properties of the samples are given in Tables I and II, respectively, where some of the original cords are first dried at 130°C for 180 sec, followed by annealing at 240°C for 120 sec (so-called heat set treatment used widely in the tyre industry), while others are further dipped in a liquid of adhesives (so-called dipped cord). The tyre cords and rubber sheets (thickness ~ 0.5 mm) after a simulated running test of about 10^5 km in the laboratory were also used, whose tensile strength and Young's modulus before and after fatigue are shown in Table II.

To investigate the fatigue resistance properties of tyre cords using TL, various original cords which have different fatigue resistances were used. The fatigue data obtained from different fatigue tests are shown in Table III.

2.2. Experiments and measuring procedure
TL measurements generally involve two operations: the irradiation by high-energy rays and the measurement of the TL glow intensity above the irradiation temperature. A detailed description of the TL measurement has been published [7, 12]. In this study the irradiation was carried out by X-ray under the conditions of 35 kV, 20 mA. The dose and the wavelength

TABLE II Mechanical properties of various PET cords used

Sample no.	TS (kg)	$E_{6.8 kg}$ (%)	E_B (%)	Shr. 150°C (%)
1	23.2	7.7	18.9	14.9
2	21.4	5.8	18.0	3.7
3	20.4	5.6	16.8	3.3
4	5.9	–	7.2	1.7

Notes: TS, tensile strength; E_B elongation at breakage point; $E_{6.8 kg}$, elongation under stress of 6.8 kg; Shr, shrinkage at 150°C.

TABLE III Various tyre cords with different fatigue resistance used in this study

No.	Sample state	Strength Retention		Fatigue index‡
		A*	B†	
9	PET 1500D/2 Original Standard Cord	87%	100%	100
10	PET 1500D/2 Original POY System Cord	96%	–	345
11	PET 1000D/2 Original POY System Cord			

*Strength retention rate is obtained by means of a disc fatigue test under ± 10% cyclic strain with 1400 r.p.m. at room temperature for 24 h.
† The same as A, except for the cyclic strain (− 10%).
‡ The fatigue index is the result of the tube fatigue test.

distribution of X-rays used were not measured because they were not essential in the present situation.

PET cords were wound on a copper sample holder while the rubber sheet, 0.5 mm thick, was cut into a rectangle of 20 mm × 18 mm to be placed on the sample holder for the TL measurement. Samples and sample holder were irradiated in air at room temperature for 2 h and then fixed in a vacuum cryostat at a pressure of 10^{-3} torr to prevent oxidation. After free emission for 45 min at room temperature, the sample was warmed up to about 450 K at a certain rate, during which the TL glow curve was continuously measured. The heating rates for all the samples used in this study are 3, 4, 6, and 12 K min⁻¹, respectively.

3. Analysis of TL activation energy, E, and frequency factor, S
The original analysis of the TL process was made by Randal and Wilkins in 1940 [13, 14]. These authors derived the equation

$$I = -K (dn/dt) = -Kn \qquad (1)$$

$$K = S \exp (-E/kT) \qquad (2)$$

where I is the total TL intensity, K is a constant, dn/dt is the time rate of change of concentration of trapped electrons, S is the attempt-to-escape frequency factor for an electron in a trap with activation energy E, k is Boltzmann's constant, and T the absolute temperature. The above equations were induced from several assumptions which were discussed in detail by Pender and Fleming [15]. In the case of polymers, it is generally assumed that the traps consist of some part of the chain themselves, e.g. small segments of the back-bone chain or pendant groups. An electron might be liberated from a trap by being "shaken" off the back-bone segment or pendant group to which it is attached, when these entities jump between equilibrium positions. Such jumping motions are commonly referred to as primary and secondary relaxations in the context of dielectric and dynamic mechanical studies [16].

Integrating Equation 1 we obtain

$$n = n_0 \exp \left[s \int_0^t \exp (-E/kT) \, dt \right] \qquad (3)$$

$$I = -\alpha (dn/dt) \qquad (4)$$

$$= \alpha Sn \exp (-E/kT)$$
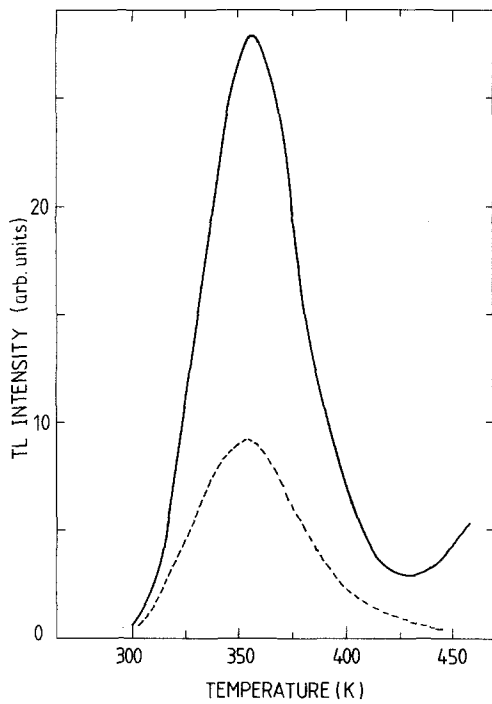
Figure 1 High-temperature TL glow curves of PET tyre cords
(- - -) before fatigue (dipped cord), (———) after fatigue.

Figure 2 High-temperature TL glow curves with different heating rates β.

In order to obtain a relation between maximum temperature, T_m, in the glow curve and heating rate, β, Hoogenstraaten's method [17] is adopted. Taking a differential against temperature T in Equation 4 and letting $dI/dT = 0$, we have

$$\exp\,(E/kT_m) \;=\; skT_m^2/E\beta \tag{5}$$

Taking logarithms on both sides of Equation 5

$$\ln\,(T_m^2/\beta) \;=\; \ln\,(E/ks) \,-\, E/kT_m \tag{6}$$

is obtained.

It can be understood from Equation 6 that the shift of the maximum temperature, T_m, is a function of the heating rate, β. A plot of $\ln\,(T_m^2/\beta)$ against $1/T_m$ should then yield a straight line with a slope of E/k and an intercept $\ln\,(E/ks)$, independent of the kinetic order of the TL mechanism. Thus from the plot shown in Equation 6, by measuring the maximum temperatures corresponding to different heating rates, β, the activation energy, E, and frequency factor, S, can be simultaneously obtained. All the data shown in the following sections are obtained by averaging the results of three or four samples.

4. Results and discussion
4.1. Correlation between E, S and fatigue of PET cords and tyre rubber

Fig. 1 shows typical high-temperature (from room temperature) TL glow curves of PET tyre cords before and after fatigue at a heating rate of 6 K min^{-1}. A sharp peak was found at about 350° K, which was related to T_g of PET, as discussed in a previous paper [7]. The shape of the glow curve in the fatigued PET cords showed almost no change compared with that of the unfatigued dipped cords. The integrated intensity, however, showed a great jump upwards after fatigue. A slight shift of the maximum towards higher temperature was also observed. In addition to the above
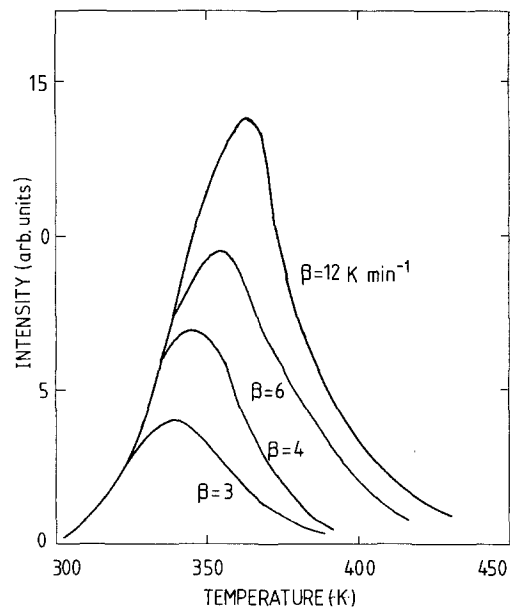
features, it should be mentioned particularly that the glow curve at a temperature higher than 420 K again rose with increasing temperature. This can be considered to be an effect of oxidation generated as fatigue proceeds, which has also been discussed before [7]. As is expressed in Equation 4, the TL integrated intensity is mainly attributed to the competing effects of the activation energy, E, and frequency factor, S. Therefore more information can be expected by elucidating the causes of the intensity jump as shown above in terms of the activation energy, E, and frequency factor, S.

Fig. 2 shows a plot of glow curves against increasing heating rate, β, as an example. The profile becomes sharper at higher heating rate and the maximum T_m subsequently shifts toward higher temperature. A plot of $\ln\,(T_m^2/\beta)$ against $1/T_m$ (see Equation 6) for PET tyre cords before and after fatigue is shown in Fig. 3 in which a good linearity of the plot can be found for heating rates of 3, 4, 6, and 12 K min^{-1}. Good linearity of the plot showed the validity of the analytical method described in this study. It is evident that the slope of the plots after fatigue in Fig. 3 is steeper than that before fatigue. The activation energy, E, is readily
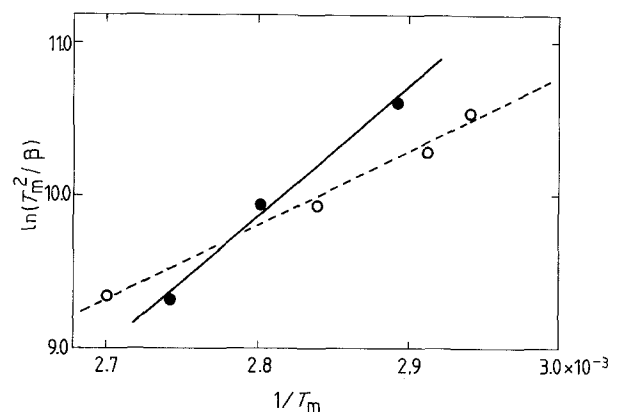

Figure 3 Ln (T_m^2/β) against $1/T_m$ plots of PET cords before and after fatigue. (- - -) Before fatigue (dipped cord); (———) after fatigue.

TABLE IV The activation energy, E, and frequency factor, S, of PET cords before and after fatigue

	Dipped (before), no. 3	After fatigue, no. 4
E (eV)	0.41	0.75
S (sec^{-1})	1.86×10^5	1.56×10^{10}

TABLE V The activation energy, E, and frequency factor, S, of the tyre rubber before and after fatigue

	Before fatigue (no.7)	After fatigue, (no.8)
E (eV)	0.58	0.64
S (sec^{-1})	6.9×10^7	2.1×10^9

calculated from the slopes of the plot in Fig. 3 and the frequency factor, S, from the intercepts.

It is worthy of note here that several methods of analysis of glow curves for the estimation of activation energy and frequency factor, proposed initially for the study of TL in inorganic materials, were applied to the investigations of polymers [18]. These methods present good justifications of their analyses for various polymers. But all of these methods, except that in this study, must assume either first-order or second-order kinetics. For this reason we adopted the method described earlier for the estimation of E and S, because of its independence of the kinetics and hence the expected higher reliability than the other methods. The values of the two parameters calculated from Fig. 3 are collected in Table IV in which those of PET dipped cords and fatigued cords are shown. The most significant feature of the results is the considerable jump in the value of S during fatigue. The value of S before fatigue was of the order of 10^5, while it showed a rapid increase after fatigue to the order of 10^{10}. In contrast to this, the increase of the activation energy was not so remarkable. This is an astonishing result because it indicates that the increase in the integrated intensity is mainly attributed to the increase in the value of the frequency factor, which reflects the enhanced mobility of the polymer back-bone chains. On the other hand, the increase of E indicates that the potential barrier of the rotation of the back-bone chains in polymers is deepened to some extent and therefore the chains or pendant groups become less flexible during fatigue. The competing effects of E and S thus produced a considerable increase in the total intensity of the glow curve.

The results obtained from tyre rubber sheet before and after fatigue shown in Fig.4 and Table V, in which the same method of analysis was used, showed the same tendency as that of PET cords, except that the
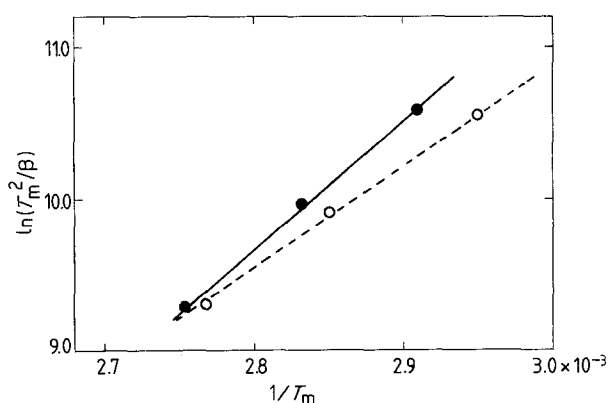
variation in the order of the value of S is not so striking as that for PET cords.

The above results are consistent with those of pulsed NMR measurements by Fujimoto [19], in which the structural changes of vulcanized rubbers filled with carbon black caused by mechanical stimuli (fatigue) has been investigated using the pulsed NMR method. The results revealed that the vulcanized rubber filled with carbon black consisted of a quasi-glassy phase (C phase) around filler particles and a liquid-like phase (A phase) away from the fillers. Each phase is changed to the more stable state by fatigue, i.e. to the more disordered state and to the more ordered state, respectively, as the system develops. As a result, the interaction of rubber molecular chains in the A-phase was weakened and the mobility was enhanced, while the interaction of molecular chains in the C-phase was enhanced and the mobility was decreased. In the present situation, although it is difficult to verify the existence of the above phases from the change of E and S directly, it can be concluded from the above results and discussion that the fatigue phenomenon in this case is intimately connected with the mobility of the molecular chains in polymers. In other words, the results imply that the variation in mobility of molecular chains is a distinguishable feature in the process of fatigue.

In addition to fatigued samples, E and S of rubber with varied vulcanizing times were also measured. Fig. 5 and Table VI give the results in which S revealed a clear dependency on vulcanizing time while the activation energy, E, remained almost unchanged. This is interesting because it seems to be analogous to the effect of annealing in which it induced a more relaxed amorphous structure that is favourable for the TL process [7].

4.2. Correlation between E, S and fatigue resistance

From the results shown in the above sections, it is

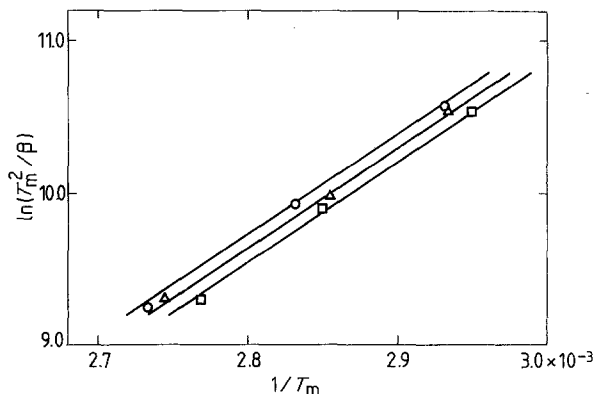*Figure 4* Ln (T_m^2/β) against $1/T_m$ plots of tyre rubber sheet before and after fatigue. (– – –) Before fatigue; (——) after fatigue.

Figure 5 Ln (T_m^2/β) against $1/T_m$ plots of rubber sheet before and after fatigue. (O) vulcanized for 15 min; (△) vulcanized for 60 min; (□) vulcanized for 120 min.

TABLE VI The activation energy, E, and frequency factor, S, of the rubber with varied vulcanizing time

Vulcanizing time (min)	E (eV)	S (10^7 sec^{-1})
15	0.58	6.43
60	0.58	6.90
120	0.58	7.40

clear that the analytical method using the plot of ln (T_m^2/β) against $1/T_m$ is very effective in showing the changes in the mobility of polymer chains during fatigue; and the activation energy, E, and especially the frequency factor, S, increase strikingly as fatigue proceeds. This suggests that S might be an adequate parameter for reflecting the fatigue resistance of polymers in some way, and therefore it is possible to correlate E and S of the materials without a preliminary fatigue test, with the fatigue resistance property, if this supposition is verified. In order to do this, two types of cords with varied fatigue resistance were measured. The sample name and their fatigue resistance data, obtained by disc and tube fatigue testing respectively, are shown in Table III. As seen, PET POY system cord (no. 10) which has improved molecular mobility (disorder) in the amorphous phase, has a better fatigue resistance compared with standard PET cord (no. 9). No. 11 is essentially the same as no. 10 except for a smaller denier number than in no. 10.

Table VII lists the activation energies and frequency factors of the various cords without preliminary fatigue testing. Nos 10 and 11, which have better fatigue resistance, showed a lower S than that of no. 9, whereas E did not exhibit such distinct changes. The results indicate that further investigations are necessary to establish a final correlation between the variations of activation energy and frequency factor with fatigue resistance performance. This is to be done in a subsequent paper.

We have shown the results of X-ray irradiated PET tyre cords before and after fatigue. But we found unexpectedly that even in the virgin form, the PET cord emitted luminescence with a maximum at about 380 K in the glow curve, as shown in Fig. 6. Three glow curves for PET original cord, PET heat set treatment cord, and PET dipped cord given together in Fig. 6. A maximum at around 380 K with a heating rate of 6 K min^{-1} was observed for original and heat set treatment cords. This reveals that some kind of trap population from the radicals generated by mechanical operations such as spinning must exist, because no glow of this kind was observed in PET fibre samples. The integrated intensity of the glow curve of the original cord decreased considerably on heat set treatment while the profile remained unchanged, except for a slight shift of the maximum towards higher tem-
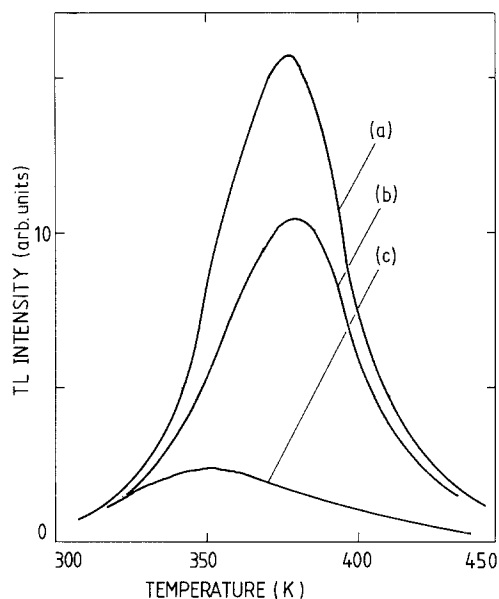

Figure 6 High-temperature TL glow curves of PET cords without X-ray irradiation. (a) Original cord; (b) heat set treatment cord; (c) dipped cord.

perature, as seen in Fig. 6. This is completely different from that observed in the annealed PET films in which the annealing enhanced the total intensity, as reported previously [7]. The calculated activation energy and frequency factor are 0.95 eV and 2.4×10^{12}, respectively, much larger than those in X-ray irradiated samples. The glow peak almost disappeared in the dipped cords. This is also interesting because it possibly reflects the distinct effects of adhesives on the fatigue resistance of tyre cords, and therefore provides new proof for the assumptions that the dipped treatment will improve the fatigue resistance of tyre cord. It is, however, more important to notice that the glow observed in the PET virgin cord is essentially different from that of X-ray irradiated samples. The TL from the X-ray irradiated samples reflects the molecular mobility, while that from virgin cord does not, and therefore must be removed.

5. Conclusion

In this paper the fatigue features and fatigue resistance of PET tyre cords, as well as tyre rubber, were investigated by means of analysis of TL activation energy and frequency factor. It was found that the activation energy, E, and frequency factor, S, both increased during fatigue, the frequency S strikingly so. The results from cords without preliminary fatigue testing but with varied fatigue resistance indicated that the changes in S and E during fatigue may be used as a sensor to detect the fatigue resistance property of polymers, although more detailed investigations, which are under way, are required.

Acknowledgement

References
1. C. E. FELTNER and J. D. MORROW, Trans. ASME Ser. D 83 (1961) 15.

TABLE VII The activation energy E and frequency factor S of various cords without fatigue

	Sample no.		
	9	10	11
E (eV)	0.69	0.65	0.64
S (sec^{-1})	3.1×10^9	7.4×10^8	1.5×10^8

2. M. HIGUCHI and Y. IMAI, *J. Appl. Polym. Sci.* **14** (1970) 2379.
3. F. OISHI, *Materials* **7** (1968) 826 (in Japanese).
4. J. A. SAUER and G. C. RICHARDSON, *Int. J. Fracture* **16** (1980) 499.
5. J. C. RADON, *ibid.* **16** (1980) 533.
6. T. KAJIYAMA, *Sen-i Gakkai-shi* **39** (12) (1983) 445.
7. L. B. LIU and K. MIYASAKA, *Polymer* **23** (1988) 286.
8. K. MIYASAKA and T. HASHIMOTO, *Sen-i Gakkai-shi* **38** (10) (1982) 72.
9. M. RUSSELL, *Br. Polym. J.* **1** (1969) 53.
10. R. ONO and N. KOMATSU, *Sen-i Gakkai-shi* **18** (11) (1962) 955.
11. R. G. PATTERSON and R. K. ANDERSON, *Rubber Chem. Technol.* **49** (1965) 832.
12. K. HIYAMA, MSc thesis, Tokyo Institute of Technology (1985).
13. J. T. RANDAL and M. H. WILKINS, *Proc. Roy. Soc.* **A184** (1939) 347.
14. *Idem, ibid.* **185** (1940) 366.
15. L. F. PENDER and R. J. FLEMING, *J. Phys. C, Solid State Phys.* **10** (1977) 1561.
16. R. H. PARTRIDGE, *J. Polym. Sci.* **A3** (1965) 2817.
17. W. HOOGENSTRAATEN, *Philips Res. Rept.* **13** (1958) 515.
18. R. J. FLEMING, *J. Polym. Sci.* **A-2 6** (1968) 1283.
19. K. FUJIMOTO, *Nihon Gomu Kyoukai-shi* **38** (10) (1965) 843.